



Queensland University of Technology
Brisbane Australia

This is the author's version of a work that was submitted/accepted for publication in the following source:

Eichmann, Troy, Khan, Razmi, McIntyre, Tim, Jacobs, Carolyn, Porat, Hadas, Buttsworth, David, & [Upcroft, Ben](#) (2011) Radiometric temperature analysis of the Hayabusa spacecraft re-entry. In *28th International Symposium on Shock Waves*, 17 - 22 July 2011, University of Manchester, Manchester.

This file was downloaded from: <http://eprints.qut.edu.au/43728/>

© Copyright 2011 [please consult the authors]

Notice: *Changes introduced as a result of publishing processes such as copy-editing and formatting may not be reflected in this document. For a definitive version of this work, please refer to the published source:*

Radiometric temperature analysis of the Hayabusa spacecraft re-entry

T.N. Eichmann¹, R. Khan², T.J. McIntyre¹, C. Jacobs², H. Porat², D. Buttsworth³, and B. Upcroft²

1 Introduction

Hayabusa, an unmanned Japanese spacecraft, was launched to study and collect samples from the surface of the asteroid 25143 Itokawa. In June 2010, the Hayabusa spacecraft completed its seven year voyage. The spacecraft and the sample return capsule (SRC) re-entered the Earth's atmosphere over the central Australian desert at speeds on the order of 12 km/s. This provided a rare opportunity to experimentally investigate the radiative heat transfer from the shock-compressed gases in front of the sample return capsule at true-flight conditions. At these conditions, the total heat transfer to the vehicle has a significant radiative component and this can be estimated by studying the radiation emitted from the shock layer and the hot surface. Such measurements can be compared with numerical simulations of the flow and with results from ground-based testing in shock tunnels and expansion tubes. This in turn leads to a better understanding of the complex thermochemistry occurring within the shock layer and aids in the design of more efficient thermal protection systems for future spacecraft.

This paper reports on the results of observations from a tracking camera situated on the ground about 100 km from where the capsule experienced peak heating during re-entry. Previously, manual tracking has been used to measure the radiative heat transfer experienced at the surface of a re-entering vehicle for the Stardust ([1], [2], [3]) and Genesis ([4]) missions. However, acquiring and tracking the vehicle is difficult and can be unreliable. In our approach, two cameras were used to record the radiative emission from the capsule. A tracking camera followed the position of the spacecraft in the sky, in turn directing a second camera instrumented with a diffraction grating to record spectral data. Although the relatively low spatial resolution of this spectrograph arrangement meant that only an integrated signal over the entire

1 The Centre for Hypersonics, School of Mathematics and Physics, The University of Queensland, Brisbane, 4072, Australia. · 2 The Centre for Hypersonics, School of Mechanical and Mining Engineering, The University of Queensland, Brisbane, 4072, Australia. · 3 Faculty of Engineering and Surveying, University of Southern Queensland, Toowoomba, 4350, Australia.

surface of the spacecraft was recorded, the captured spectra allows the possibility of reconstructing the temperature evolution over the course of the reentry manoeuvre.

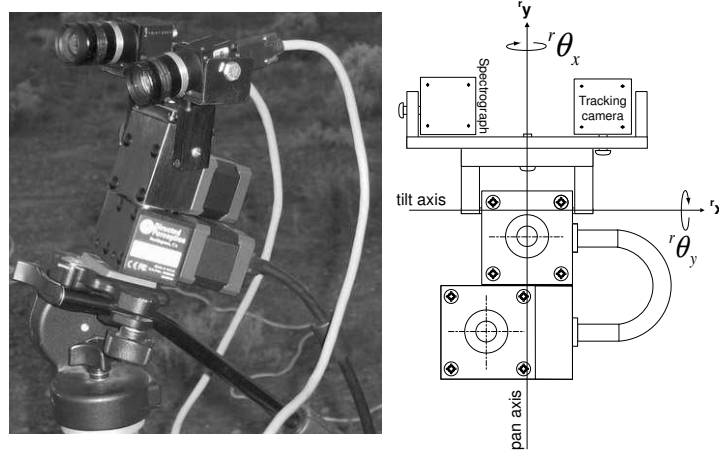


Fig. 1 A photograph and schematic diagram of the robot, spectrograph and tracking camera used during the Hayabusa re-entry

2 Instrumentation

2.1 Tracking Camera

The purpose of the Ground Observation Robotic Tracker (GORT) was to record the emission spectra of the high temperature gas in the shock layer and from the surface of the heat shield as the spacecraft, and in particular the sample return capsule, entered Earth's atmosphere. GORT consists of a Directed Perception PTU-47-17 high speed pan and tilt unit. This unit hosts two identical Point Grey Flea 2 greyscale CCD cameras sampling at a video frame rate of 22.25 Hz. One camera uses a 25mm lens and was converted to a spectrograph by the addition of an in-line 300 lines/mm transmission grating placed before the optics. The second camera has a 6mm lens and is used to robustly maintain the alignment of the instrument with the position of the vehicle using an automated image-based visual servoing approach. Optical flow techniques are used in conjunction with classical visual feedback control to track the object on the image plane and maintain the desired robot orientation. Figure 1 shows the mounting of these cameras with the tracking camera on the right and the spectrometer on the left of the robot payload bracket. A typical desktop CPU interfaces to the camera and robot using an IEEE 1394b standard interface and serial communication respectively. Two additional hard drive disks were included in the

host computer to save simultaneously streamed images from both cameras. All vision processing and robot movement tasks were handled by a C program written in Microsoft Visual Studios in a Windows-based environment.

2.2 Spectrograph Design and Calibration

The spectrograph consisted of a camera with a transmission grating attached before the lens, optimized for the near infrared (NIR) with a peak efficiency at 700nm. The dispersion of the grating and its distance from the CCD allowed wavelengths in the range 450-900nm to be recorded on the CCD array with a resolution of 0.48nm/pixel. To allow maximum wavelength resolution, the CCD was mounted on its side so that the largest dimension of the CCD array corresponded to wavelength. To obtain linear dispersion of the spectrometer and the response of the camera, the equipment was calibrated using a halophosphate phosphor fluorescent lamp and a low pressure sodium lamp to obtain wavelength calibration and an Optronic Laboratories OL200M standard source to determine the relative spectral sensitivity of the camera. In each case, the lamp was imaged from a distance of about 30 m using the identical camera/ diffraction grating arrangement used in the Hayabusa observation.

2.3 Observation

The Hayabusa capsule entered the atmosphere shortly before midnight on Sunday June 13, 2010. The radiation from the capsule was visible to the naked eye for ground-based observers in Tarcoola, Coober Pedy and surrounds for a period of about 30 seconds. Peak heating occurred at 23:22:19 local time or 13:52:19 UT. The camera was mounted on the ground at Tarcoola giving an almost front-on view of the entry capsule from a distance of approximately 140 km at peak heating. At this point, the capsule was at an altitude of about 56 km. Observation of the capsule was complicated by the fact that the capsule was close to the larger main bus from which it had just detached. This larger structure provided significant background radiation in the earlier stages of re-entry before finally burning up around peak heating. Analysis of the images required the separation of the spectra of the flow over the capsule from other background sources. Several thousand frames of images were recorded as the capsule passed through the atmosphere. However, due to space limitations only the analysis for a single frame recorded two seconds before peak heating is presented here.

3 Results

Figure 2 shows a sample intensity calibration image and a sample image from the capsule entry. The wavelength range for each is around 400-900 nm. The calibration lamp image is devoid of spectral features, showing only a smooth intensity variation characteristic of this type of lamp. In contrast, the flight image shows a clear black body radiation background, most likely from the hot surface of the vehicle. Superimposed on this profile are spectral lines from the hot gas flowing over the body and spectral holes from absorption due to the cold atmosphere between the vehicle and the ground-based camera.

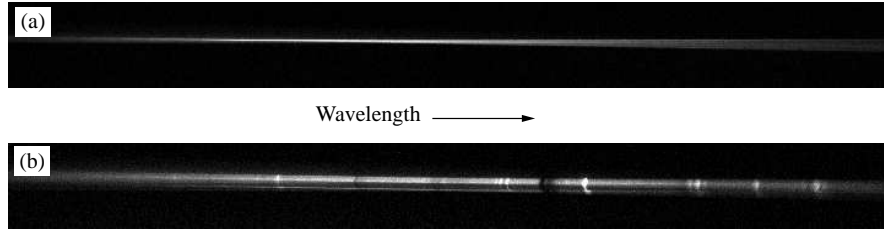


Fig. 2 Raw uncalibrated images from (a) the calibration lamp and (b) spacecraft entry.

To analyse the flight data, we first determine the spectral sensitivity of the camera/diffraction grating system. Each image shown in Fig. 2 was calibrated for wavelength. The signal from the intensity calibration image was then integrated along the spatial (vertical) axis to provide the counts at each wavelength as shown in Fig. 3a. A background subtraction was applied to remove any ambient light or offset on the camera. Then, by using the known spectral irradiance of the calibration lamp at a distance of 0.5 m from the lamp, $I(\lambda)$, a spectral sensitivity factor, $C(\lambda)$ (energy per count per unit wavelength) can be defined as

$$C(\lambda) = \frac{I(\lambda) \times t_L \times A_L \times (0.5/d)^2}{counts} \quad (1)$$

where t_L is the exposure time for the calibration image, A_L is the capture area of the lens on the camera and d is the distance of the lamp from the camera in metres. This calibration factor is seen in Fig. 3b. It shows that the spectral response of the camera system is fairly uniform across the range 500 - 800 nm becoming only less sensitive above and below this region.

A similar process is applied in the analysis of the flight image. The signal is first integrated in the spatial (vertical direction) and the background removed to obtain a raw spectrum. This is shown in Fig. 4a. The spectral radiance, $L(\lambda)$, can then be calculated by

$$L(\lambda) = \frac{counts \times C(\lambda)}{t_f} \times \frac{d_f^2}{A_L} \times \frac{1}{A_f} \quad (2)$$

Here t_f is the exposure time of the camera while recording images during the flight, d_f is the distance from the camera to the capsule, and A_f is the cross-sectional surface area of the vehicle that is observed by the camera. At present, an accurate value for the distance to the vehicle as a function of time is not available, and hence the spectral radiance will be quoted as a normalised value. This result for the image shown in Fig. 2 is given in Fig. 4b. Apparent is the increase in intensity towards the infra-red with a peak somewhere between 800-900 nm. Also apparent are the various spectral emission and absorption lines. The $H\alpha$ line at about 650 nm results from water present in the hot flow over the vehicle while both oxygen and nitrogen atoms are also observed. Absorption due to molecular oxygen and water vapour in the air is also present.

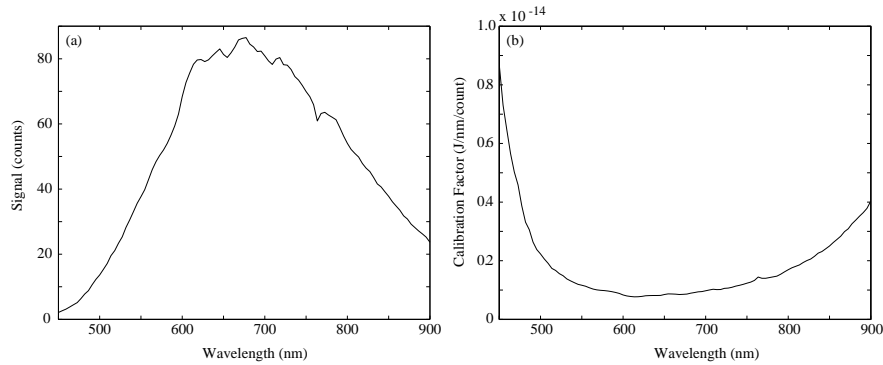


Fig. 3 Intensity calibration. (a) Counts recorded for the spectral lamp; (b) Calibration factor for the camera.

It is possible to fit a black body radiation curve to these results. Such a curve, calculated for a black body temperature of 3,200 K is shown in the figure. There is generally a good fit between the black body curve and the experimental measurements. Further work is required to determine the uncertainty in this value.

4 Conclusion

Radiometric imaging has been successfully performed on the Hayabusa spacecraft as it entered the atmosphere. A relatively simple spectrograph was designed and operated to record spectra from the hot flow and radiating surface. Automated control ensured that the capsule was tracked throughout its re-entry. The system was calibrated to allow identification of radiating species in the flow and also to make comparisons with black body curves. A temperature of around 3,200 K was measured in this analysis. Work is continuing in an attempt to make a comparison between the absolute level of the spectral radiance determined from the analysis and that

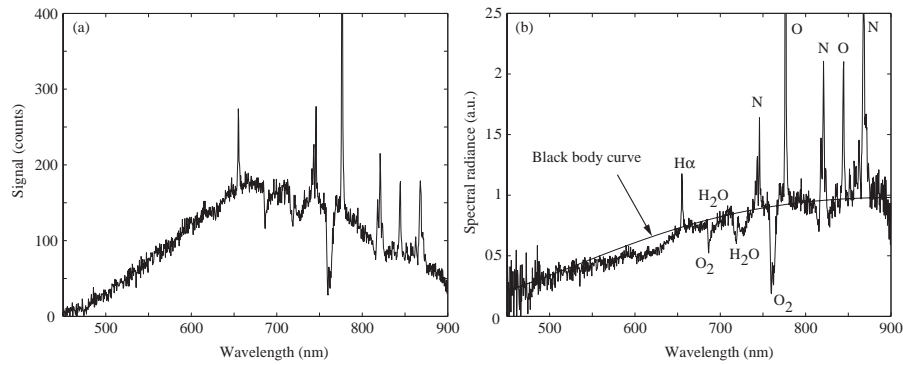


Fig. 4 Flight data. (a) Raw spectrum; (b) Normalised spectral radiance shown with a black body curve calculated for a surface with a temperature of 3,200 K.

given off by a black body. Further work is also underway to investigate the spectral properties of the emission lines and to process the many other images that were obtained.

5 Acknowledgements

The authors would like to acknowledge the contributions made by the technical staff at the University of Queensland and the University of Southern Queensland. Financial assistance was also provided by both institutions to allow equipment preparation and for travel.

References

1. Winter, M. et al. Spectroscopic Observations of the STARDUST Re-Entry in the Near UV. 39th AIAA Thermophysics Conference, Miami, FL, AIAA 2007-4050. (2007)
2. McHarg, M. G. et al. Observation of the STARDUST Sample Return Capsule Entry using a High Frame Rate Slit-less Spectrograph. 46th AIAA Aerospace Sciences Meeting and Exhibit, Reno, Nevada, AIAA 2008-1211. (2008)
3. Jenniskens, P. Observations of the STARDUST Sample Return Capsule Entry with a Slit-less Echelle Spectrograph. 46th AIAA Aerospace Sciences Meeting and Exhibit, Reno, Nevada. (2008)
4. Jenniskens, P. et al. Surface Heating from Remote Sensing of the Hypervelocity Entry of the NASA Genesis Sample Return Capsule. 44th AIAA Aerospace Sciences Meeting and Exhibit, Reno, Nevada. (2006)